

THE EFFECT OF GENE FLOW ON COALESCENT-BASED SPECIES-TREE INFERENCE

COLBY LONG AND LAURA KUBATKO

ABSTRACT. Most current methods for inferring species-level phylogenies under the coalescent model assume that no gene flow occurs following speciation. While some studies have examined the impact of gene flow on estimation accuracy for certain methods (e.g., [6, 4, 16]), limited analytical work has been undertaken to directly assess the potential effect of gene flow across a species phylogeny. In this paper, we consider a three-taxon isolation-with-migration model that allows gene flow between sister taxa for a brief period following speciation, as well as variation in the effective population sizes across the tree. We derive the probabilities of each of the three gene tree topologies under this model, and show that for certain choices of the gene flow and effective population size parameters, anomalous gene trees (i.e., gene trees that are discordant with the species tree but that have higher probability than the gene tree concordant with the species tree) exist. We characterize the region of parameter space producing anomalous trees, and show that the probability of the gene tree that is concordant with the species tree can be arbitrarily small. We then show that the SVDQuartets method is theoretically valid under the model of gene flow between sister taxa. We study its performance on simulated data and compare it to two other commonly-used methods for species tree inference, ASTRAL and MP-EST. The simulations show that ASTRAL and MP-EST can be statistically inconsistent when gene flow is present, while SVDQuartets performs well, though large sample sizes may be required for certain parameter choices.

INTRODUCTION

Nearly all of the currently-used methods for coalescent-based estimation of species trees assume that speciation occurs at a precise instant of time, with immediate cessation of gene flow, and that gene flow between distinct species elsewhere on the phylogeny does not occur. While several studies have examined the impact of gene flow on the performance of species-level phylogenetic inference (e.g., [6, 4, 16]), analytic analyses of the potential impact of gene flow are limited, despite the development of mathematical tools that could facilitate such study (e.g., [10, 1, 24]). Recently, Tian and Kubatko (2016) considered a three-species IM (isolation-with-migration) model [9, 8, 25] that allowed gene flow between sister species, and derived the probability distribution of gene tree topologies and gene tree histories under this model. Their work generalized the work of Zhu and Yang (2012), who considered a similar model but with gene flow allowed only between the terminal sister taxa. Both Zhu and Yang (2012) and Tian and Kubatko (2016) used their results to estimate model parameters via maximum likelihood. Zhu and Yang (2012) considered sequence data arising from the model, while Tian and Kubatko (2016) considered the observed distribution of gene tree histories.

Though Tian and Kubatko (2016) included some exploration of the effect of different choices of parameters on the gene tree topology distribution, they focused on cases of symmetric migration in which the species tree satisfied the molecular clock and in which the effective population size (which determines the rate of coalescence) in each branch was the same. Under those conditions, they found that the gene tree topology that matched the species tree occurred with probability at least as large as the other two gene tree topologies. In other words, there were no *anomalous gene trees* [5] in this case. The assumption of common effective population sizes is implicitly made in some species tree estimation methods [17], while Bayesian approaches (e.g., [7]) generally include inference of separate effective population size parameters in the posterior distribution

they estimate. However, the effect of variation in the rate of coalescence on the distribution of gene tree topologies has not been carefully examined, in either the presence or the absence of gene flow (note that Degnan and Salter (2005) also assumed the same effective population sizes in all branches of the species tree).

Here, we consider the distribution of gene tree topologies for a three-species IM model that generalizes that considered by Tian and Kubatko (2016) to include time periods with and without gene flow between both pairs of sister species. We further consider the effect of variation in population sizes and migration rates on this distribution. We mathematically derive explicit conditions under which anomalous gene trees do exist, and show that, in fact, the probability of the gene tree topology that matches the species tree can be made arbitrarily small. We then consider the impact of these results on several of the commonly-used methods for species tree inference under the multispecies coalescent, including SVDQuartets [2], ASTRAL [20], and MP-EST [17]. We show that SVDQuartets is theoretically valid under our general model, while ASTRAL and MP-EST appear to be statistically inconsistent in the presence of gene flow for some choices of parameters. We compare the performance of all three methods using simulation for multilocus data, and additionally assess the performance of SVDQuartets for coalescent independent sites. We begin by carefully defining our model.

A GENERAL IM MODEL FOR THREE SPECIES

Isolation-with-migration (IM) models have a long history in the population genetics literature [9, 8, 25], and have more recently been considered in the context of species tree estimation [26, 24]. Here we consider a more general version of the IM model than that presented in [24]. Figure 1a shows a species tree with three species, labeled A , B , and C , with topology $((A, B), C)$. We assume that we have sampled one lineage from each species, and these lineages are labeled with lowercase letters a , b , and c . Within each population on the species tree, θ_X denotes the effective population size parameter, which determines the rate of coalescence, in the branch that represents species X ($X = A, B, C$, or AB , with θ_{AB} denoting the size of the population ancestral to species A and B). The parameter τ_1 indicates the time from the present to the speciation event separating species A and B , and τ_2 indicates the time from the present to the speciation event separating the ancestral species AB from species C . Following each speciation event (looking forward in time), there is a time period over which migration occurs, indicated by blue shading in Figure 1a. The length of this time period of gene flow between species A and B is $t_{A \leftrightarrow B}$ and the length of the period of gene flow between the ancestor of A and B and species C is $t_{AB \leftrightarrow C}$. Thus, there are two intervals of time during which there is no gene flow (complete isolation), of lengths $\tau_1 - t_{A \leftrightarrow B}$ and $(\tau_2 - \tau_1) - t_{AB \leftrightarrow C}$. Finally, we define the rates of gene flow between species as m_j , where $j = 1$ for gene flow from AB to C , $j = 2$ for gene flow from C to AB , $j = 3$ for gene flow from A to B , and $j = 4$ for gene flow from B to A (looking backward in time).

We are interested in computing the probabilities of the three possible gene tree topologies for different choices of the parameters defined above ($\theta_A, \theta_B, \theta_{AB}, \theta_C, m_1, m_2, m_3, m_4, t_{A \leftrightarrow B}, t_{AB \leftrightarrow C}, \tau_1$, and τ_2). We use lowercase letters a , b , and c to denote lineages sampled from species A , B , and C , respectively, in the three possible gene trees. The gene tree that matches the species tree is denoted by $((a, b), c)$, and will be referred to as the *concordant topology* (CT). The two *discordant topologies* (DT) are then $((b, c), a)$ and $((a, c), b)$. We begin by considering the effect of gene flow between the sister species A and B . If there is any gene flow between these two species then there are only two possible outcomes. First, the two lineages a and b could coalesce in either population A or B , leading to a gene tree that matches the species tree. Second, the lineages could fail to coalesce during the time over which A and B are separate species, resulting in both a and b entering the ancestral interval. Varying the values of θ_A, θ_B, m_3 and m_4 will affect the probabilities of observing each of these outcomes, but regardless, it is impossible for coalescent

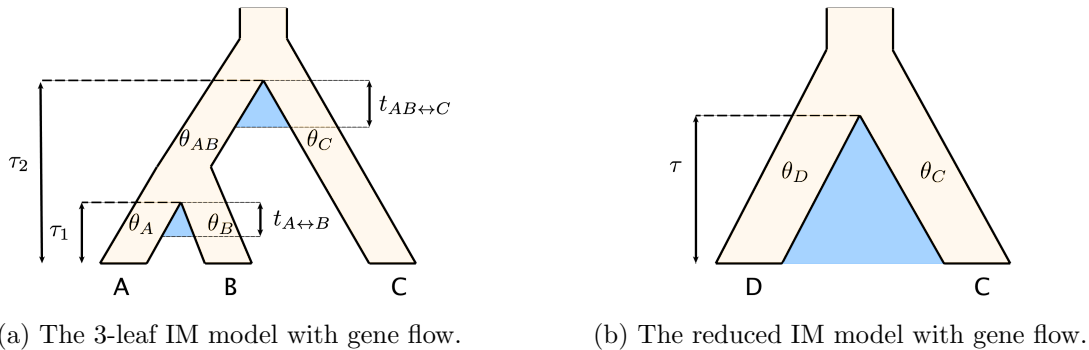


FIGURE 1. The species tree parameters of the IM model with gene flow and the reduced IM model.

events leading to discordant gene trees to occur before time τ_1 . Likewise, for any fixed choice of θ_A, θ_B, m_3 and m_4 , increasing τ_1 will lead to a larger proportion of gene trees that match the species tree, while decreasing it will have the opposite effect. In either case, it is impossible to obtain a gene tree discordant with the species tree as a result of any event that occurs before time τ_1 .

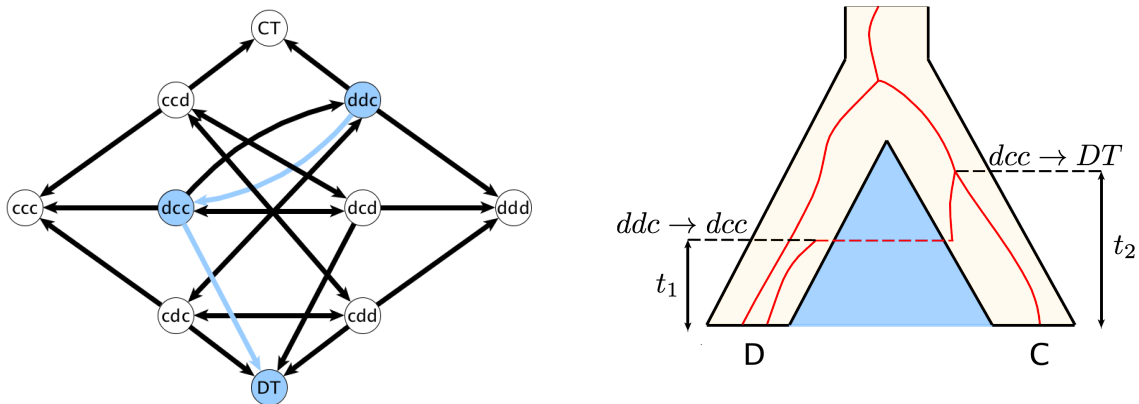
In order to understand the formation of anomalous gene trees, we will carefully analyze the second case in which a and b do not coalesce before τ_1 and enter the ancestral interval. This allows us to study a reduced model with only two species, C and D , where D represents the ancestor of A and B and contains two lineages, a and b . In addition, since no discordant gene trees can form in the interval of no gene flow between population AB and population C , we will exclude this interval. The reduced model over which we carry out calculations is depicted in Figure 1b, where for simplicity we have labeled the time from the present to the speciation event τ and the population size for population D by θ_D . The migration parameters m_1 and m_2 are defined as before. We note that the model in Figure 1b can be thought of as a limiting case, obtained when $(\tau_2 - \tau_1) - t_{AB \leftrightarrow C} \rightarrow 0$ and $m_3 = m_4 = 0$. All of the results that we derive below can be straightforwardly extended to the model in Figure 1a. We return to this point in the discussion at the end of the paper.

To compute gene tree topology probabilities under the model in Figure 1b, we use the approach introduced by Hobolth et al. (2011) in which we define a continuous-time Markov chain whose states are assignments of lineages to populations. For example, the “starting state” of our reduced Markov process (i.e., the state at the present time) is represented by ddc . What we mean by this is that the lineage sampled from species A is in species D , the lineage sampled from species B is in species D , and the lineage sampled from species C is in species C . In general, position in the string xyz will denote whether we are referring to the lineage sampled from A , B , or C , respectively, and the letter assigned (c or d) will indicate which species the lineage is a member of at the particular time under consideration.

A sequence of transitions between states corresponds to a *gene tree history*, a term used by both [5] and [24] to denote the sequence and relative timing of a set of coalescent events that generate a gene tree. However, since we are only interested in the gene tree topology, not the specific history that produced that topology, we will not need to keep track of the specific populations in which coalescent events occur. Instead, since the first coalescent event uniquely determines the topology of the gene tree that forms, we will introduce two absorbing states to the Markov chain that describes our model. These states, CT and DT , correspond to the formation of concordant triples and discordant triples. For example, suppose we begin in state ddc and that the lineage sampled in species B migrates to species C at time t_1 . Then we will have observed a transition of the Markov chain from state ddc to state dcc . If the lineages in C

then coalesce at time t_2 , then a discordant triple will eventually form. Therefore, the Markov chain transitions from state dcc to the state DT . This sequence of transitions is depicted in Figure 2.

Once we have defined the Markov chain, we can compute the *transition probabilities* for the reduced IM model, the probability that the chain transitions from any state to any other state over the time interval of length τ . Since we are particularly interested in the gene tree topology frequencies and since our chain always begins in state ddc , we are most interested in the probabilities of transition from state ddc to states CT and DT . Notice, however, that some gene tree must form even if no coalescent event occurs in the gene flow interval. If no coalescent event occurs over the gene flow interval, then the Markov chain ends in one of the states ccc , ccd , cdc , dcc , ddc , dcd , or ddd , and all three lineages enter the population ancestral to C and D . In such a case, the probability of each gene tree topology forming is equal to $1/3$. Therefore, knowing all of the transition probabilities will allow us to determine the probability of a concordant triple or discordant triple forming in the reduced IM model. By symmetry in the model, the two discordant topologies form with equal probability, and so we can compute each gene tree topology probability explicitly. However, there is one further observation that we may make to reduce the complexity of the Markov chain representing the reduced IM model. That is that once the chain enters either state ccc or ddd , the probability of each gene tree topology forming is now $1/3$, and we do not need to keep track of any other subsequent transitions. Thus, for simplicity, we can treat ccc and ddd as absorbing states.



(a) The Markov chain of the reduced IM model.

(b) The species tree of the reduced IM model.

FIGURE 2. A particular sequence of coalescent and migration events in the reduced IM model and the corresponding path in the Markov chain. The chain starts in state ddc (shaded circle in (a) and depicted at the present time (i.e., at the tips of the tree) in (b)). At time t_1 , the lineage sampled from B migrates between D and C , as depicted in (b) with a dotted horizontal line. This is represented in (a) by a transition from state ddc to state dcc (blue arrow). At time t_2 , the lineages sampled from B and C coalesce in C , which is a transition from dcc to DT (blue arrow in (b)).

Figure 2a depicts the Markov chain of the reduced IM model with arrows representing the possible transitions between states under the assumption that only a single event can happen at a given instant of time (i.e., two or more events do not happen at precisely the same instant of time). The instantaneous transition rates are the parameters of the model we described above, and the instantaneous rate matrix is given by,

$$Q = \begin{array}{c} \begin{array}{cccccc|cccc} & ddc & dcd & cdd & ccd & cdc & dcc & ddd & ccc & CT & DT \\ ddc & -- & 0 & 0 & 0 & m_1 & m_1 & m_2 & 0 & \alpha_D & 0 \\ dcd & 0 & -- & 0 & m_1 & 0 & m_1 & m_2 & 0 & 0 & \alpha_D \\ cdd & 0 & 0 & -- & m_1 & m_1 & 0 & m_2 & 0 & 0 & \alpha_D \\ \hline ccd & 0 & m_2 & m_2 & -- & 0 & 0 & 0 & m_1 & \alpha_C & 0 \\ cdc & m_2 & 0 & m_2 & 0 & -- & 0 & 0 & m_1 & 0 & \alpha_C \\ dcc & m_2 & m_2 & 0 & 0 & 0 & -- & 0 & m_1 & 0 & \alpha_C \\ \hline ddd & 0 & 0 & 0 & 0 & 0 & 0 & 0 & 0 & 0 & 0 \\ ccc & 0 & 0 & 0 & 0 & 0 & 0 & 0 & 0 & 0 & 0 \\ CT & 0 & 0 & 0 & 0 & 0 & 0 & 0 & 0 & 0 & 0 \\ DT & 0 & 0 & 0 & 0 & 0 & 0 & 0 & 0 & 0 & 0 \end{array} \end{array}$$

where $\alpha_C = 2/\theta_C$ and $\alpha_D = 2/\theta_D$ are the rates of coalescence in populations C and D , respectively. In the next section, we explain how to use the instantaneous rate matrix Q to compute the transition probabilities over the interval τ to derive explicit formulas for the probabilities of the three gene tree topologies.

ANALYTIC RESULTS FOR THE ISOLATION WITH MIGRATION MODEL

In this section, we derive an explicit formula for the probability of observing a gene tree concordant with the species tree in the reduced IM model described above. As noted previously, since the other two gene tree topologies occur with equal probability, this allows us to determine the probability of each gene tree topology. To obtain this formula, we must exponentiate the product of the rate matrix Q and the parameter τ in terms of the parameters to obtain the transition probabilities [14]. In general, computing the exponential of a matrix in terms of the parameters is difficult, even for relatively small matrices. However, the number of absorbing states in our simplified model allows us to write the rate matrix Q as a block matrix with two zero blocks. This will enable us to give explicit formulas for entries of the matrix exponential, and consequently, to obtain an explicit formula for the probability of observing the concordant triple.

To compute the probability of observing a concordant triple in the reduced IM model, we will consider the two possible ways that one might form. One way is for the Markov chain to transition from state ddc to state CT during the interval of gene flow of length τ in the species tree. The other way for a concordant triple to form is for the Markov chain to transition from ddc to any state other than CT or DT along the interval of gene flow. As noted above, conditional on this event, the concordant triple will form with probability $1/3$, since all three lineages entered the same branch during the interval of gene flow or will enter the same branch CD at the end of the interval of gene flow. Thus, the concordant triple frequency as a function of the rate matrix is given by,

$$(1) \quad F(\alpha_C, \alpha_D, m_1, m_2, \tau) = \exp(Q\tau)_{ddc,CT} + \frac{1}{3}(1 - \exp(Q\tau)_{ddc,CT} - \exp(Q\tau)_{ddc,DT}).$$

To expand the formula above in terms of the parameters, we only require two entries of the transition matrix. Rewriting the rate matrix Q in block form will enable us to write the matrix exponential in terms of submatrices of Q . For the following proposition, let $Q = \begin{pmatrix} M & N \\ 0 & 0 \end{pmatrix}$ where

$$M = \begin{pmatrix} -- & 0 & 0 & 0 & m_2 & m_2 \\ 0 & -- & 0 & m_2 & 0 & m_2 \\ 0 & 0 & -- & m_2 & m_2 & 0 \\ 0 & m_1 & m_1 & -- & 0 & 0 \\ m_1 & 0 & m_1 & 0 & -- & 0 \\ m_1 & m_1 & 0 & 0 & 0 & -- \end{pmatrix} \text{ and where } N = \begin{pmatrix} m_2 & 0 & \alpha_D & 0 \\ m_2 & 0 & 0 & \alpha_D \\ m_2 & 0 & 0 & \alpha_D \\ 0 & m_2 & \alpha_C & 0 \\ 0 & m_2 & 0 & \alpha_C \\ 0 & m_2 & 0 & \alpha_C \end{pmatrix}.$$

Proposition 0.1. *For any $\tau \in \mathbb{R}$ and generic choices of rate matrix parameters $\alpha_C, \alpha_D, m_1,$ and $m_2,$*

$$\exp(Q\tau) = \begin{pmatrix} \exp(M\tau) & ((\exp(M\tau) - I)M^{-1}N) \\ 0 & 0 \end{pmatrix}.$$

Proof. Recall that the formula for the matrix exponential is given by

$$\exp(Q\tau) = \sum_{i=0}^{\infty} \frac{(Q\tau)^i}{i!} = I + Q\tau + \frac{(Q\tau)^2}{2!} + \dots,$$

and by induction, for $i \geq 1,$ $(Q\tau)^i = \begin{pmatrix} (M\tau)^i & M^{i-1}\tau^i N \\ 0 & 0 \end{pmatrix}.$ Therefore, the upper left block of $\exp(Q\tau)$ is simply equal to $\exp(M\tau).$ We also have

$$\begin{aligned} \exp(M\tau) &= I + M\tau + \frac{M^2\tau^2}{2!} + \frac{M^3\tau^3}{3!} + \dots \\ (\exp(M\tau) - I) &= M\tau + \frac{M^2\tau^2}{2!} + \frac{M^3\tau^3}{3!} + \dots \\ (\exp(M\tau) - I)M^{-1}N &= \tau N + \frac{M\tau^2 N}{2!} + \frac{M^2\tau^3 N}{3!} + \dots, \end{aligned}$$

and this last line is exactly the upper right block of $\exp(Q\tau).$ \square

The formula for the probability of observing the concordant triple depends only on two entries from the upper right block of the transition matrix $\exp(Q\tau).$ To compute these entries, we must first compute the 6×6 matrix $\exp(M\tau).$ For a generic choice of nonnegative parameters, the matrix M has only four distinct eigenvalues but can be diagonalized so that $M = PAP^{-1},$ where Λ is the diagonal matrix of the eigenvalues of $M.$ Thus, $\exp(M\tau) = P\exp(\Lambda\tau)P^{-1}.$ Similarly, for a generic choice of nonnegative parameters we can write the entries of M^{-1} explicitly, and simplify to write the concordant triple frequency as

$$\begin{aligned} F(\alpha_C, \alpha_D, m_1, m_2, \tau) &= -(1/3)(-2fm_1^2 - 2fm_2^2 + fe_1\alpha_D m_1 + 2fe_1\alpha_D m_2 + fe_2\alpha_C \alpha_D - fe_2\alpha_C m_1 + \\ & fe_2\alpha_D m_1 + 2fe_2\alpha_D m_2 - e_1\alpha_C \alpha_D m_1 + 3e_1\alpha_C \alpha_D m_2 - 3e_1\alpha_C m_1 m_2 + e_1\alpha_D m_1 m_2 + \\ & e_2\alpha_C \alpha_D m_1 - 3e_2\alpha_C \alpha_D m_2 + 3e_2\alpha_C m_1 m_2 - e_2\alpha_D m_1 m_2 + fe_1\alpha_C \alpha_D - fe_1\alpha_C m_1 - \\ & 4fm_1 m_2 + e_1\alpha_C^2 \alpha_D - e_1\alpha_C^2 m_1 - e_1\alpha_C \alpha_D^2 - 3e_1\alpha_C m_1^2 - e_1\alpha_D^2 m_1 - \\ & 2e_1\alpha_D^2 m_2 - e_1\alpha_D m_1^2 + 2e_1\alpha_D m_2^2 - e_2\alpha_C^2 \alpha_D + e_2\alpha_C^2 m_1 + e_2\alpha_C \alpha_D^2 + \\ & 3e_2\alpha_C m_1^2 + e_2\alpha_D^2 m_1 + 2e_2\alpha_D^2 m_2 + e_2\alpha_D m_1^2 - 2e_2\alpha_D m_2^2 - 3f\alpha_C \alpha_D - \\ & f\alpha_C m_2 - 3f\alpha_D m_1 - 6f\alpha_D m_2)/ \\ & ((\alpha_C \alpha_D + 2\alpha_C m_1 + \alpha_C m_2 + \alpha_D m_1 + 2\alpha_D m_2 + 2m_1^2 + 4m_1 m_2 + 2m_2^2)f) \end{aligned}$$

where

$$\begin{aligned}
 g &= -\frac{1}{2}(\alpha_C + \alpha_D + 3m_1 + 3m_2) \\
 f &= (\alpha_C^2 - 2\alpha_C\alpha_D - 2\alpha_Cm_1 + 2\alpha_Cm_2 + \alpha_D^2 + 2\alpha_Dm_1 - 2\alpha_Dm_2 + m_1^2 + 2m_1m_2 + m_2^2)^{1/2} \\
 e_1 &= \exp((g + f/2)\tau) \\
 e_2 &= \exp((g - f/2)\tau).
 \end{aligned}$$

All of the parameters of the model are nonnegative real numbers and the formula is valid and well-defined for a generic choice of parameters. The Maple file to verify this formula is contained in the Supplementary Materials. There, we also give an example to show that this formula agrees with the output from the COALGF software [24] for the concordant triple frequency.

Characterizing the Gene Flow Anomaly Zone. With this formula in hand, we can state a number of propositions about the concordant triple frequency and identify various regions of parameter space that produce anomalous behavior. Here, we define the *gene flow anomaly zone* to be the region of parameter space for which the concordant triple frequency is less than $1/3$. We note again that by the symmetry of the lineages a and b in the reduced IM model, the two discordant triple frequencies are always given by $\frac{1}{2}(1 - F(\alpha_C, \alpha_D, m_1, m_2, \tau))$. The following proposition shows that this model is flexible enough to produce any concordant triple frequency.

Proposition 0.2. *For any $\gamma \in (0, 1)$ there exists a choice of parameters $(\alpha_C, \alpha_D, m_1, m_2, \tau) \in \mathbb{R}_{\geq 0}^5$ such that $F(\alpha_C, \alpha_D, m_1, m_2, \tau) = \gamma$.*

Proof. For fixed $m_1 > 0$, setting $\alpha_C = \tau$ and $\alpha_D = m_2 = 1/\tau$, $\lim_{\tau \rightarrow \infty} F(\alpha_C, \alpha_D, m_1, m_2, \tau) = 0$. Similarly, for fixed $\alpha_C, \alpha_D > 0$, if $m_1 = m_2 = 1/\tau$, then $\lim_{\tau \rightarrow \infty} F(\alpha_C, \alpha_D, m_1, m_2, \tau) = 1$. \square

Intuitively, discordant triples are very likely to form when we allow unidirectional gene flow from population D to population C , reduce the probability of coalescence in population D , and then impose a very high rate of coalescence in C . Since lineages a and b are unlikely to coalesce in D , given enough time, eventually one of these lineages will flow into population C and immediately coalesce with lineage c to produce a discordant triple. While this scenario gives insight into what conditions might produce anomalous behavior, it is not actually a requirement that the rate of gene flow from D to C be greater than the rate from C to D (i.e., that $m_1 > m_2$). In [24], the authors analyzed a model with equal rates of gene flow, (i.e., where $m_1 = m_2$) and showed the concordant triple frequency could be made very close to $1/3$. In fact, the following proposition shows that even with this restriction, the concordant triple frequency can be made to approach $1/9$.

Proposition 0.3. *For any $\gamma \in (\frac{1}{9}, 1)$ there exists a choice of parameters $(\alpha_C, \alpha_D, m, m, \tau) \in \mathbb{R}_{\geq 0}^5$ such that $F(\alpha_C, \alpha_D, m, m, \tau) = \gamma$. Moreover, for any choice of parameters $(\alpha_C, \alpha_D, m, m, \tau) \in \mathbb{R}_{\geq 0}^5$, $1/9 \leq F(\alpha_C, \alpha_D, m, m, \tau) \leq 1$.*

Proof. From the initial state ddc , the sum of the instantaneous rates of change to the states ddd and CT is greater than $1/3$ the total rate of change to all other states. Once the system is in either ddd or CT , the probability of a concordant triple forming is at least $1/3$. Therefore, $F(\alpha_C, \alpha_D, m, m, \tau) \geq \frac{1}{9}$.

For fixed $m_1 = m_2 > 0$, setting $\alpha_C = \tau$ and $\alpha_D = 1/\tau$, $\lim_{\tau \rightarrow \infty} F(\alpha_C, \alpha_D, m_1, m_2, \tau) = 1/9$. Similarly, for fixed α_C and $\alpha_D > 0$, if $m_1 = m_2 = 1/\tau$ then $\lim_{\tau \rightarrow \infty} F(\alpha_C, \alpha_D, m_1, m_2, \tau) = 1$. \square

Figure 3 shows a region of parameter space with $m_1 = m_2$ which produces anomalous gene trees and where the concordant triple frequency approaches the limiting value of $1/9$. Whether

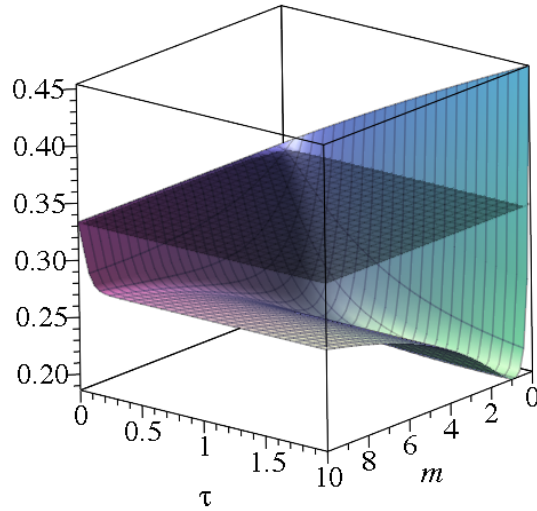


FIGURE 3. A plot of the concordant triple frequency from the reduced IM model as a function of the length of the interval of gene flow (τ) and the symmetric rate of gene flow ($m = m_1 = m_2$). The other parameters of the model are fixed at $\alpha_C = 10$ and $\alpha_D = 0.1$. Note that everywhere the surface is below the shadowed plane is a region of parameter space producing anomalous gene trees.

or not the gene flow rates are equal, one essential feature for producing anomalous behavior is that the rate of coalescence in population C must be greater than that in population D . The following proposition makes this relationship between the coalescence parameters formal.

Proposition 0.4. *For any fixed $\alpha'_C, \alpha'_D > 0$, there exists an $m'_1, m'_2, \tau' \in \mathbb{R}_{\geq 0}$ such that $F(\alpha'_C, \alpha'_D, m'_1, m'_2, \tau') < 1/3$ if and only if $\alpha'_C > \alpha'_D$.*

Proof. For all $\alpha_C, \alpha_D, m_1, m_2 > 0$, $F(\alpha_C, \alpha_D, m_1, m_2, 0) = 1/3$ and $\frac{\partial F}{\partial \tau}(0) = 2\alpha_D/3 > 0$. There is at most one point for which $\frac{\partial F}{\partial \tau}(s) = 0$, which implies that if there exists m'_1, m'_2, τ' such that $F(\alpha'_C, \alpha'_D, m'_1, m'_2, \tau') < 1/3$, it must be that $\lim_{\tau \rightarrow \infty} F(\alpha'_C, \alpha'_D, m'_1, m'_2, \tau) < 1/3$. Evaluating the limit and solving, we see that $\lim_{\tau \rightarrow \infty} F(\alpha_C, \alpha_D, m_1, m_2, \tau) < 1/3$ if and only if $2\alpha_C\alpha_D + 2\alpha_Dm_1 + 4\alpha_Dm_2 - 2\alpha_Cm_1 < 0$. \square

Corollary 0.5. *For any fixed $\alpha'_C, \alpha'_D > 0$, there exists an $m', \tau' \in \mathbb{R}_{\geq 0}$ such that $F(\alpha'_C, \alpha'_D, m', m', \tau') < 1/3$ if and only if $\alpha'_C > 3\alpha'_D$.*

SPECIES TREE ESTIMATION IN THE PRESENCE OF GENE FLOW

There are several phylogenetic estimation methods that reconstruct species tree topologies under the coalescent model using the observed frequencies of estimated gene tree topologies. These so-called *summary methods* (or sometimes, *summary statistics methods* [18]) take advantage of the fact that for the coalescent model on an unrooted quartet tree, the most probable gene tree topology is that concordant with the species tree. By choosing an outgroup, these methods can be applied to infer the rooted topology of a 3-leaf species tree under the coalescent model. However, as we have just shown, in the presence of gene flow, the most common gene tree topology may not be that concordant with the species tree topology. As was also noted in [22], the summary methods will be positively misleading in such cases. By contrast, in this section we show that the method of SVDQuartets remains theoretically valid in the presence of

gene flow. We offer here a brief review of the method which suggests why it should be effective on data produced by the IM model with gene flow described in this paper.

Theoretical Justification for the Performance of SVDQuartets. The method of SVDQuartets is applied to sequence data generated under the multispecies coalescent in order to infer the unrooted species tree topology [2]. The method works by using singular value decomposition to infer the unrooted topology of the induced 4-leaf subtrees of the species tree, also called *quartets*, which are then assembled to reconstruct the unrooted species tree. The method of inferring quartets is statistically consistent and can be combined with any exact algorithm for reconstructing species trees from quartets to yield a statistically consistent method of inferring species trees under the coalescent model.

In this section we offer some justification for why SVDQuartets is still an effective method for inferring the species tree under the three-species IM model with gene flow. By selecting an outgroup, we can use SVDQuartets to infer the rooted topology of a 3-leaf species tree under the coalescent model. With the outgroup added, the 4-leaf species tree of the model is an equidistant, rooted caterpillar, and we label the cherry of this tree by A and B . The symmetry in the cherry of the species tree implies that $p_{i_1 i_2 i_3 i_4} = p_{i_2 i_1 i_3 i_4}$, where $p_{i_1 i_2 i_3 i_4}$ is the probability of observing the DNA site pattern $i_1 i_2 i_3 i_4$, $i_j \in \{A, C, G, T\}$, $j = 1, 2, 3, 4$, at the tips of the species tree under the coalescent model. For the purposes of this paper, it will suffice to know that producing a probability distribution that satisfies these linear relationships is a sufficient but not necessary condition for SVDQuartets to correctly infer the unrooted topology of the 4-leaf species tree with unlimited data. We omit the full details of the SVDQuartets method here and refer the reader instead to [3]. Because of the outgroup, the rooted species tree can be assumed to be a rooted caterpillar, and so the unrooted topology uniquely determines the rooted 3-leaf species tree. Our claim is that the expected site pattern probabilities from the three-species IM model with gene flow also satisfy these same linear relationships, implying that SVDQuartets is still valid in the presence of gene flow.

That the three-species IM model with gene flow satisfies these linear relationships follows simply by the symmetry between A and B in the model in the case where the rates of gene flow and coalescence between A and B are the same (i.e., $m_3 = m_4$ and $\theta_A = \theta_B$). If $m_3 \neq m_4$ or $\theta_A \neq \theta_B$, then the argument is only slightly more involved. We divide the gene trees into two sets, those that involve a coalescent event in either A or B and those that do not. The first set of gene trees are all concordant with the species tree. By the symmetry in the cherry of each concordant gene tree, the site pattern probabilities produced by each of these gene trees satisfies $p_{i_1 i_2 i_3 i_4} = p_{i_2 i_1 i_3 i_4}$, and so must the sum of the site pattern probabilities from all of these gene trees. For the second set of gene trees, each of the two lineages a and b both enter the population AB . While the site pattern probabilities from each individual gene tree will not necessarily satisfy these relationships, the indistinguishability of the lineages a and b upon entering population AB guarantees that the sum of the site pattern probabilities from all of these gene trees will satisfy $p_{i_1 i_2 i_3 i_4} = p_{i_2 i_1 i_3 i_4}$, regardless of the values of m_1 and m_2 . Since the site pattern probabilities at the tips of the species tree under the three-species IM model are the sum of the site pattern probabilities from these two sets of gene trees, they must also satisfy $p_{i_1 i_2 i_3 i_4} = p_{i_2 i_1 i_3 i_4}$. To formally prove the validity of SVDQuartets under this model requires a more detailed justification of these relationships and verification that the discordant topologies do not satisfy these relationships. Further, the result can be extended to the case in which the species tree does not satisfy the molecular clock, following the argument in [19].

Performance of Reconstruction Methods in the Presence of Gene Flow. Given the result above that indicates that SVDQuartets is theoretically valid in the presence of gene flow, we assess the performance of the method under various conditions using simulation. For all of the simulations described here, the four-taxon model tree is shown in Figure 4, with speciation

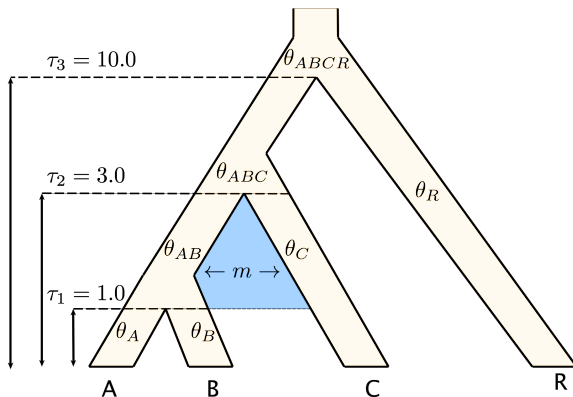


FIGURE 4. Model tree for the simulation studies.

times given by $\tau_1 = 1.0$, $\tau_2 = 3.0$, and $\tau_3 = 10.0$, in coalescent units. The choice of a large interval between the second and third speciation events was made so that the gene tree topology distribution would mimic that of the three-taxon case described above. Because the interval $\tau_3 - \tau_2$ is long, we expect lineages a , b , and c to coalesce completely within this interval with high probability. Thus the tree can be viewed as being rooted by taxon R . We use this model tree to carry out two distinct sets of simulation studies that differ in the types of input data used. We describe each simulation set-up and the corresponding results separately below.

Coalescent Independent Sites. Our first simulation study involves the generation of data consisting of *coalescent independent sites*. Coalescent independent sites are sampled by first simulating some number, n , of gene trees under the model in Figure 4. For each of the n gene trees, a single site is generated according to one of the standard nucleotide substitution models. This results in a dataset consisting of n sites that are conditionally independent given the species tree. This simulation setting is designed to mimic SNP data, except that there is no requirement that sites are variable or that they include only two alleles. In other words, any site pattern can be included in the dataset, but all sites are independently generated under the model, conditional on the species tree. Within the setting of coalescent independent sites, we consider three distinct sets of simulations designed to assess the performance of SVDQuartets under different scenarios. The first setting involves conditions under which anomalous gene trees exist due to the presence of gene flow and varying θ parameters. In particular, we fix $\theta_A = \theta_B = \theta_C = \theta_R = \theta_{ABC} = \theta_{ABCR} = 2.0$ and set $\theta_{AB} = 20.0$. This amounts to slowing the rate of coalescence in population AB , which results in migration out of this population before coalescence of lineages a and b with fairly high probability, leading to an increase in the proportion of discordant gene trees. We assume no gene flow between species A and B (i.e., $m_3 = m_4 = 0$), and allow symmetric gene flow between populations AB and C at rate m (i.e., we set $m_1 = m_2 = m$). We vary m to assess performance of SVDQuartets at varying levels of gene flow. Gene genealogies are simulated using the software `ms` [12] with the command line: `./ms 4 n -t 2.0 -T -I 4 1 1 1 1 -ej 0.5 1 2 -ej 1.5 2 3 -ej 5.0 3 4 -em 0.5 2 3 m/2 -em 0.5 3 2 m/2 -en 0.5 2 20.0 > treefile`, where $m = 0, 0.4, 0.8, 1.2, 1.6, 2.0, 4.0$, or 8.0 . In the units used by `ms`, $m = 2Np$, where p is the fraction of population AB made up of migrants from population C at each generation (and similarly for C and AB since we assume symmetric migration) and N is the effective population size. Once the gene genealogies are generated, a single site is evolved along each genealogy using the software `Seq-Gen` [21] under either the JC69 model [13] (command: `./seq-gen -s 0.025 -q -mHKY`) or the GTR+I+G model [23] (command: `./seq-gen -s 0.025 -q -mGTR -r 1.0 0.2`

10.0 0.75 3.2 1.6 -f 0.15 0.35 0.15 0.35 -i 0.2) for

$n = 10,000; 50,000; 100,000; 200,000; 400,000; 600,000; 800,000; 1,000,000.$

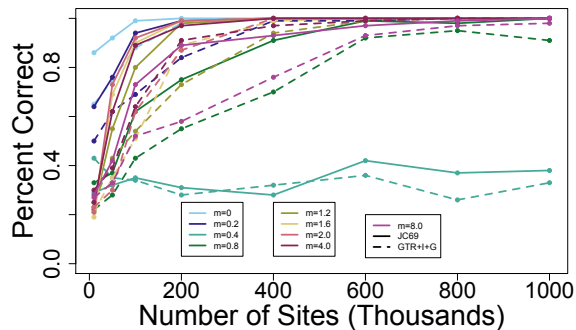
At each setting for m and n and for each substitution model, 100 data sets are simulated, and the proportion of data sets for which the correct four-taxon tree is estimated is recorded.

The next simulation setting we consider within the context of coalescent independent sites is designed to assess the impact of changing the θ parameters in the presence of moderate levels of gene flow. Holding m fixed at 0.8, we considered $\alpha_C = 5.0, 10.0,$ and 20.0 (recall that $\theta_C = 2/\alpha_C$). The corresponding command in `ms` was `./ms 3 n -t 2.0 -T -I 3 1 1 1 -ej 0.5 1 2 -ej 1.5 2 3 -n 3 w -em 0.5 2 3 0.4 -em 0.5 3 2 0.4 -en 0.5 2 y > treefile`, where in this command, the parameters (\mathbf{w}, \mathbf{y}) took values $(0.1, 50.0)$, $(0.05, 200.0)$, and $(0.025, 800.0)$. For comparison, we include the case where $\alpha_C = 1.0$, which corresponds to the Simulation 1 setting for which $m = 0.8$. All other settings were the same as in the previous simulation. Finally, we considered a collection of settings for which there are no anomalous gene trees, but for which all three gene trees have somewhat similar probabilities. The only change from the first simulation study is to set $\theta_{AB} = 4.0$ (instead of 20.0).

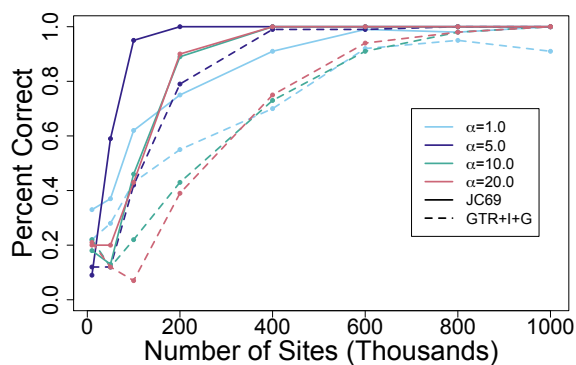
Results of Coalescent Independent Sites Simulations. The results of the first set of simulation studies using coalescent independent sites are shown in Figure 5a for data simulated with both the JC69 model (solid lines) and the GTR+I+G model (dotted lines). We first note that, in general, as the number of sites increases, the accuracy of SVDQuartets increases as well, with accuracy at or near 100% for 1,000,000 sites. While this is true for most levels of gene flow (m), even for the largest m considered ($m = 8.0$), it does not appear to be true for the intermediate value $m = 0.4$, where the accuracy appears to fluctuate around 1/3 across all sample sizes.

We investigated this unexpected result in two ways. First, the theory above tells us that SVDQuartets is theoretically valid for all values of m , and so, with enough data, the method should be able to accurately infer the species tree. Thus, we repeated the simulation with $n = 10,000,000$ bp, and found that SVDQuartets recovered the correct tree 79% of the time for the JC69 model and 61% of the time for the GTR+I+G model. These results suggest that there is some feature of this model that makes inferring the species tree under these conditions more difficult, in the sense that more data are required for accurate inference. Our second approach was therefore to try to understand why this might be the case. We considered the predicted frequencies of the gene tree histories (computed using the COALGF software [24]) in the context of the theory in the previous section that shows the validity of SVDQuartets. In particular, we note that the signal for inferring the species tree comes from the expected equality of site patterns $p_{i_1 i_2 i_3 i_4}$ and $p_{i_2 i_1 i_3 i_4}$, but that many different histories provide observations of these site patterns. For this choice of parameters, the particular histories that carry most of the information about the species tree occur in very low frequency, and thus large sample sizes are required for the signal to become definitive. While this choice of parameters is especially difficult for SVDQuartets in that more data are required for good performance, the range of these “bad” parameter choices appears to be narrow, since the setting $m = 0.2$ (navy lines in Figure 5a) and $m = 0.8$ (dark green lines in Figure 5a) both show good performance.

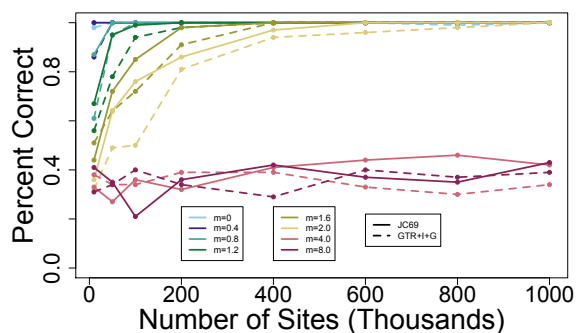
Our next observation from the results displayed in Figure 5a is that, in general, when data are simulated under the GTR+I+G model, more data are needed to achieve a given level of accuracy. This is reasonable, since more complicated models may require more data for accurate inference. Finally, we note that as m increases, the method again requires more data for accurate inference (with the exception noted above). While the values of n (the number of coalescent independent sites) considered here are large, many of those sites will be constant or non-informative. To emphasize this, Figure 6 shows histograms of the number of variable sites (Figures 6a and c) and number of parsimony informative sites (Figures 6b and d) for the cases where $m = 0$ and where $m = 2.0$. When $m = 0$, the mean proportion of variable sites across 100 replicates under



m	Prob(CT)	Prob(DT)
0.0	0.4542	0.2729
0.2	0.3347	0.3326
0.4	0.3023	0.3488
0.8	0.2963	0.3518
1.2	0.3020	0.3490
1.6	0.3071	0.3465
2.0	0.3109	0.3445
4.0	0.3206	0.3397
8.0	0.3264	0.3368



α_C	Prob(CT)	Prob(DT)
1.0	0.2963	0.3518
5.0	0.2133	0.3933
10.0	0.1864	0.4068
20.0	0.1690	0.4155



m	Prob(CT)	Prob(DT)
0.0	0.7547	0.1226
0.2	0.5497	0.2251
0.4	0.4635	0.2683
0.8	0.3988	0.3006
1.2	0.3755	0.3122
1.6	0.3641	0.3179
2.0	0.3574	0.3213
4.0	0.3447	0.3276
8.0	0.3387	0.3307

FIGURE 5. Results of the simulation studies using coalescent independent sites. In each row, the figure on the left shows the number of coalescent independent sites on the x-axis, and the accuracy (percent correct trees in 100 replicates) on the y-axis. The solid lines show results for the JC69 model, while the dotted lines show results for the GTR+I+G model. The table to the right gives the probability of the concordant and discordant topologies for the values of the parameter being varied in that simulation. Row (a): Simulation 1 varies m for $\theta_{AB} = 20.0$; Row (b): Simulation 2 varies α_C for $m = 0.8$; Row (c): Simulation 3 varies m for $\theta_{AB} = 4.0$.

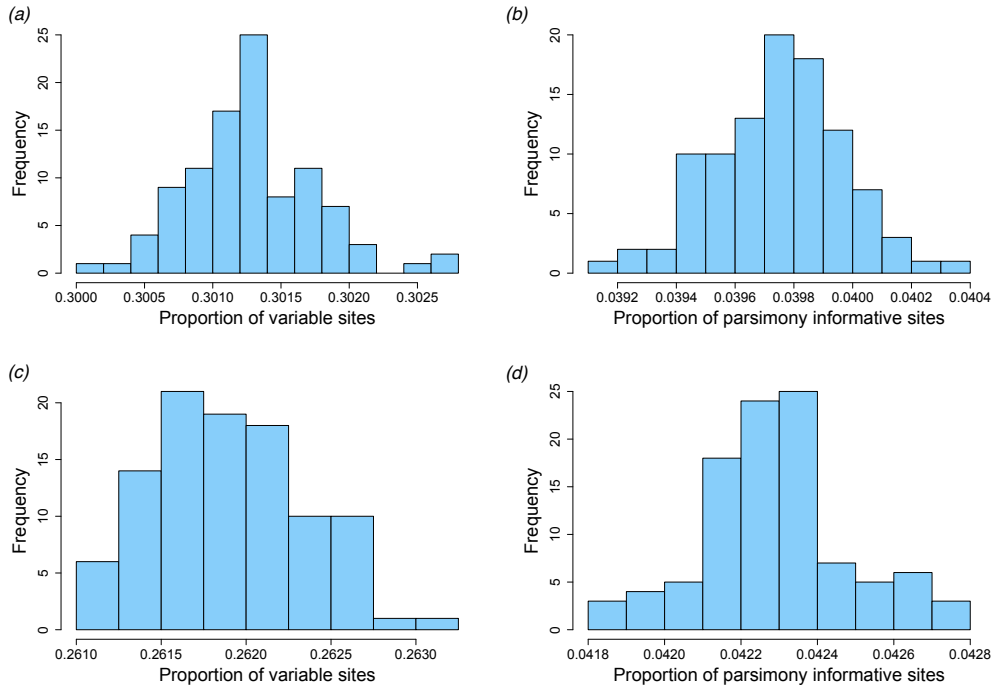


FIGURE 6. Proportion of variable sites (a and c) and parsimony-informative sites (b and d) for the coalescent independent sites simulations under the JC69 model when $m = 0$ (a and b) and when $m = 2.0$ (c and d).

the JC69 model was 30.13%, and the mean proportion of parsimony-informative sites was 3.97%. When $m = 2.0$, the mean proportion of variable sites was 26.19%, and the mean proportion of parsimony-informative sites was 4.23%. Thus, the number of SNPs required (using the standard definition of SNPs) would be much lower than the values of n considered here.

The results of the second simulation study, in which population sizes are varied while m is fixed at 0.8, are shown in Figure 5b. The general observations in this case are the same as above. In particular, as the sample size n increases, the accuracy of the method increases as well, with accuracy at or near 100% for the largest sample sizes considered. Also, the accuracy for data simulated under the GTR+I+G model is lower at a fixed n than for those simulated under JC69, a finding not unexpected given that GTR+I+G is a more complicated model than JC69. Finally, we point out that SVDQuartets is successful even in the case of extreme incongruence. For example, for the largest α_C considered ($\alpha_C = 20.0$), the probability of the gene tree topology that matches the species tree is only 16.9%, while each of the other two gene tree topologies have probability 41.55%. Thus, though fewer than 20% of the data points are obtained from the gene tree matching the species tree, SVDQuartets is able to recognize the patterns in the data once a sufficient amount of data are observed and correctly infer the species tree with high accuracy.

In the third simulation study using coalescent independent sites, there are no anomalous gene trees; instead, the probabilities of each of the three gene trees are relatively similar, with the probability of the gene tree that matches the species tree a little bit larger. The results of this simulation are shown in Figure 5c, and indicate that the same basic patterns of the previous

simulations are maintained. Specifically, accuracy increases with n and decreases as we move from the simpler model (JC69) to the more complex model (GTR+I+G). We also note that accuracy decreases as m increases, indicating that the addition of gene flow to the model makes it more difficult to infer the correct species tree. However, for all but the largest values of gene flow ($m = 4.0$ and $m = 8.0$) the accuracy is over 90% with 400,000 or more sites, while for $m = 4.0$ and $m = 8.0$, the accuracy is only around 30% at all levels of n considered. This level of gene flow perhaps represents the case where the extent of genetic exchange between populations is large enough that a species tree cannot be determined when all three trees are observed with approximately equal frequency. Interestingly, however, in the first simulation study, these high levels of gene flow did not hinder accurate estimation. We conjecture that the signal in the case of anomalous gene trees in the first simulation study makes it easier to identify the correct species tree, whereas in this case, all three trees appear in near equal frequency. In addition, the role of the mutation process and distribution of coalescent times likely play a role in determining the difficulty of the inference problem, and these are more difficult to examine. However, the theory above does indicate that with enough data, SVDQuartets should be able to accurately infer the species tree, even when the level of gene flow is high. To examine the issue in more detail, we repeated the simulation for $m = 8.0$ with $n = 10,000,000$ sites for the JC69 model, and found that the proportion of correctly estimated trees had risen to 54%, compared to 39% when $n = 1,000,000$, indicating that with sufficient data, the method can correctly recover the species tree.

Multilocus Data. We repeat all three of the simulation studies described above in the setting in which multilocus data, rather than coalescent independent sites, have been collected. The first step of each simulation is the same as described above: the `ms` software is used to simulate a set of gene trees from the model species tree in Figure 4. The number of gene trees simulated, denoted G , will correspond here to the number of genes, and we consider G ranging from 200 to 3,000 in increments of 200. Then, for each gene tree, an alignment of 300bp is simulated using Seq-Gen, with the same settings as above. As before, 100 replicates at each simulation setting are generated. We analyze each simulated multilocus data set with SVDQuartets, as well as with two other software packages designed to estimate species trees from multilocus data under the coalescent model, ASTRAL [20] and MP-EST [17]. As mentioned above, both ASTRAL and MP-EST are summary methods that work by first estimating gene trees for each gene, and then looking for subtrees that appear most frequently in the set of estimated gene trees. ASTRAL uses (unrooted) quartet frequencies across gene trees to find the species tree, while MP-EST considers rooted triples. In either case, we expect that ASTRAL and MP-EST will have difficulty in estimating the species tree in the presence of anomalous gene trees, because incorrect relationships will appear at highest frequency across the genes in this case. In our simulations, we use PAUP* to estimate the gene trees using maximum likelihood with the GTR+I+G model with all parameters estimated. In the case of ties in the likelihood score, we randomly keep one of the tied trees using the PAUP* option `keepone=random`. The gene trees estimated by PAUP* are used as input into ASTRAL and MP-EST.

Results of the Multilocus Simulations. The results of the first multilocus simulation are shown in Figure 7a and 7b for the JC69 model and GTR+I+G model, respectively, for varying m . First, we note that the accuracy of SVDQuartets (solid lines) is similar to that of Simulation 1 for the coalescent independent sites data, except that the number of sites required to achieve the same accuracy in the multilocus setting is larger. This is because, for example, 600 sites sampled from 2 genes (300bp per gene, as in our multilocus simulation study) give less information about the species tree than 600 sites sampled from 600 gene trees (as in our coalescent independent sites simulations). The 600 sites observed from 600 distinct gene trees give independent genealogical information about the species tree, though indirectly, while the 300 sites for each of the two

genes can give a reasonable indication of the individual gene trees, but still provide only two observed gene genealogies.

Next, we note that the number of genes needed to achieve a given level of accuracy is larger for the GTR+I+G model than for the JC69 model, similar to what was observed for the coalescent independent sites simulations. Comparing the performance of ASTRAL and MP-EST with SVDQuartets, we see that all three methods perform well when there is no gene flow or when the level of gene flow is low ($m = 0.2$), with ASTRAL and MP-EST outperforming SVDQuartets when the number of genes is not too large. However, as the amount of gene flow increases, both ASTRAL and MP-EST have accuracy that decreases to 0% as the number of genes increases, as expected. It is interesting to note that the unusual portion of the parameter space that was observed in the coalescent independent sites simulations (i.e., $m = 0.4$) exists here as well – and all three methods struggle to obtain accurate inference at smaller sample sizes under this setting. We maintain the same explanation as above for the performance of SVDQuartets, and note that we expect the accuracy of SVDQuartets to increase as the data size increases. To test this, we repeated our simulation with 50,000 genes of length 300bp under the JC69 model, and observed that 60% of the species tree were accurately estimated, supporting our explanation that larger sample sizes are need for more challenging problems. However, it is somewhat puzzling that ASTRAL and MP-EST do as well as they do in this case, since the gene tree that matches the species tree should be estimated less frequently than the other two gene trees. We conjecture that this results from an interaction between the mutation process and the process of generating the gene genealogies, and that this effect would disappear if longer (i.e., > 300 bp), more informative genes were generated. We note that our observation is similar to other observations in which species trees in the anomaly zone do not necessarily lead to inconsistent inference, while those outside the anomaly zone may [15, 11]. In other words, the anomaly zone is not the only predictor of performance of species tree inference methods; rather, the mutation process also plays an important role.

The results of the second multilocus simulation study are shown in Figure 7c (JC69 model) and 7d (GTR+I+G model) when m is fixed at 0.8 and α_C varies. Since there are anomalous gene trees in this case, we expect ASTRAL and MP-EST to perform poorly, and this is in fact what is observed. Their accuracy goes to 0% quickly for all choices of α_C . SVDQuartets also behaves as expected, with accuracy increasing to 100% as sample size, in this case, the number of genes, increases, for all choices of α_C .

The results of third multilocus simulation study are shown in Figures 7e (JC69 model) and 7f (GTR+I+G model). Recall that in this case, there are no anomalous gene trees, but that the three gene tree topologies occur in relatively equal frequency. For both the JC69 and the GTR+I+G models, all three methods perform well when the level of gene flow is not too high ($m \leq 2.0$), but their performance deteriorates when $m = 4.0$ or $m = 8.0$. These results are consistent with what was observed for the coalescent independent sites data.

DISCUSSION

Our goals in this paper are two-fold: first, to understand how gene flow affects the distribution of gene tree topologies under the coalescent; and second, to assess how gene flow impacts the accuracy of species tree estimation methods. Towards the first goal, we have shown that in a simple 3-taxon species tree, the combination of gene flow and variation in effective population sizes across the tree can result in anomalous gene trees. Under a simplified model in which gene flow occurs only between ancestral sister populations, we derived the probability of obtaining a gene tree concordant with the species tree, and characterized the *gene flow anomaly zone*, the regions of parameter space in which the two discordant gene trees each have higher probability than that of the concordant gene tree. Our results show that when asymmetric migration rates are allowed, the probability of the concordant topology can be made arbitrarily small, while the

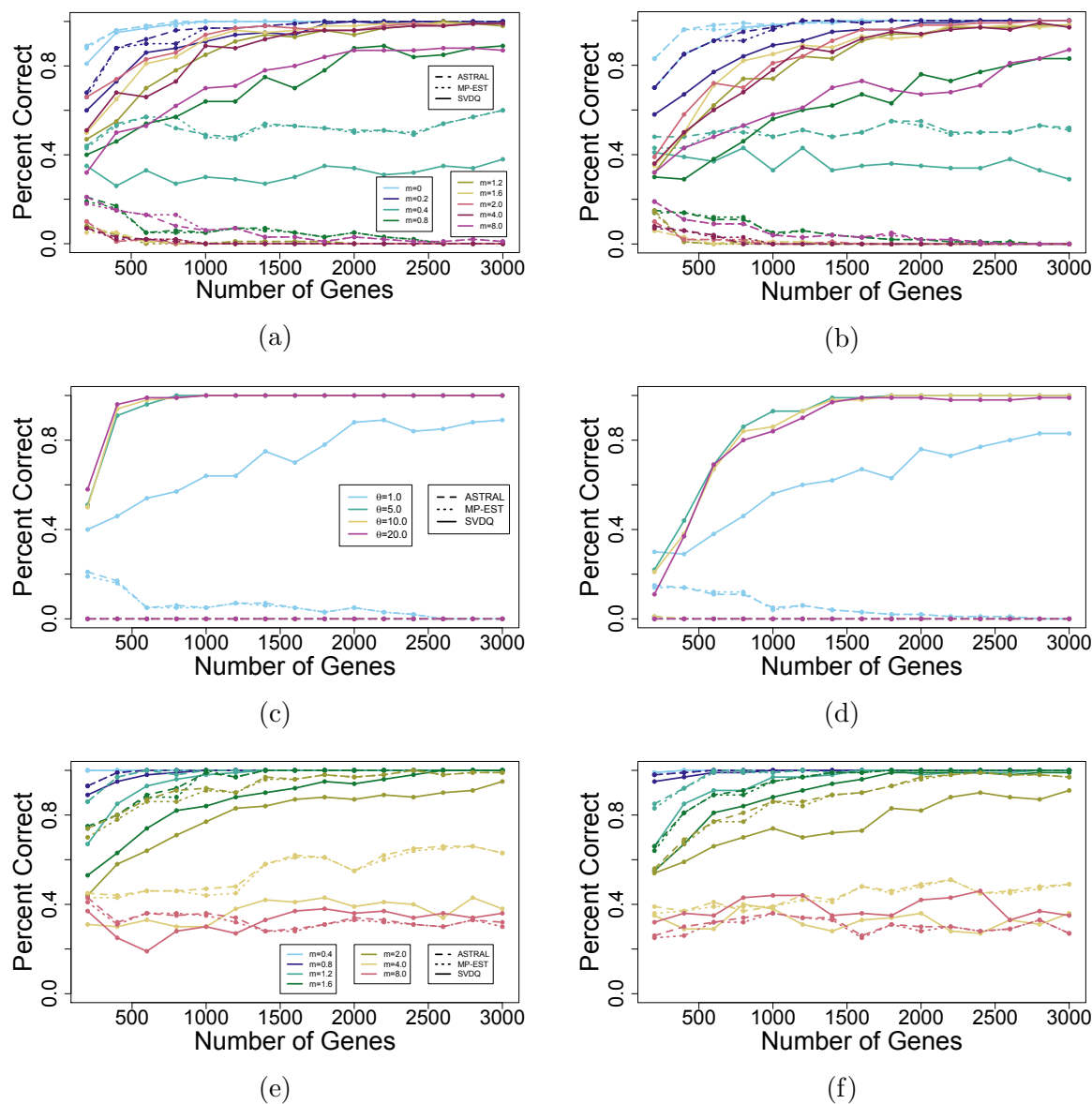


FIGURE 7. Results of the multilocus simulation study. The rows give the results of simulations 1, 2, and 3, respectively, while the left column gives results for the JC69 model and the right column gives results for the GTR+I+G model. In each graph, the x-axis gives the number of genes, each 300bp in length, and the y-axis shows the percent of trees correctly estimated in 100 replicates. Parameter settings for simulations 1, 2, and 3 are as in Figure 5.

probabilities of each of the two discordant topologies approach 50%. However, when symmetric gene flow is assumed, the probability of the concordant topology is bounded below by $1/9$, with values between $1/9$ and $1/3$ resulting in anomalous gene trees. In addition, in the case of symmetric gene flow, we found that the rate of coalescence in the recipient population must be more than 3 times as large as that of the donor population (looking backward in time) for anomalous gene trees to exist under this simplified model.

Figure 3 highlights that, though the model is simple, the gene flow anomaly zone can be fairly complicated due to the interaction between the migration rate parameters and the population sizes. The lengths of the speciation intervals also play a role, as these interact with the coalescent rate to determine the probability with which coalescent events occur within specific populations on the species tree. While our results apply directly to the reduced IM model from Figure 1b, we can extend these to conclude that there are still anomalous gene trees in the full 3-taxon IM model in Figure 1a. The main differences between these models is that the 3-taxon IM model includes an interval of gene flow between populations A and B and an interval of no gene flow between populations AB and C . During each of these intervals, the only coalescent events possible are those leading to a gene tree that is concordant with the species tree. Thus, with all other parameters fixed, the probabilities of the concordant topology will increase as the length of either of these intervals increases (with a corresponding decrease in the proportion of discordant topologies). Still, as the length of these intervals goes to zero, the model approaches the reduced IM model and there will be choices of parameters producing anomalous gene trees. Of course, if the interval of gene flow between populations A and B is decreased and the interval of no gene flow between populations AB and C is increased, the model approaches the standard model with no gene flow, for which it is known that there are no anomalous gene trees.

Towards our second goal, we argued that SVDQuartets is a theoretically valid method in the presence of gene flow and supported this result with simulation studies. For example, even in the case in which the probability of the concordant tree was only $\sim 17\%$ (see Figure 5b), SVDQuartets correctly inferred the species tree with over 95% accuracy for 400,000 coalescent independent sites under the JC69 model, and for 800,000 coalescent independent sites for the GTR+I+G model. While SVDQuartets shows similar accuracy when multilocus data are simulated, ASTRAL and MP-EST often perform poorly in the gene flow anomaly zone, with accuracy decreasing to 0% as the number of genes increases. This is to be expected in a sense, because both ASTRAL and MP-EST are based on models that assume immediate cessation of gene flow following speciation and constant effective population size. Our simulations thus indicate that these methods can be extremely sensitive to violations of these assumptions.

Certain model conditions were difficult for all three of the methods. In particular, very high rates of gene flow resulted in poor accuracy for all methods with 3,000 genes, even for parameter choices outside of the gene flow anomaly zone. This observation is consistent with studies of the performance of species tree estimation methods in the anomaly zone [15, 11], for which it has been observed that there is also an important effect of the mutation process on accuracy. We also note that in the presence of very high levels of gene flow, it may even be argued that species should not actually be considered distinct. But even in these situations, it is reassuring that with sufficient data, SVDQuartets can overcome the conflicting signal in the data and correctly infer the true relationships.

The model in Figure 1a is of particular interest, because it represents the biologically plausible scenario in which speciation occurs with subsequent gene flow between populations for some period of time, which may be more realistic than speciation with instantaneous cessation of gene flow. This was our rationale for focusing on a model that only allowed gene flow between sister populations for a specific time following speciation. The fact that SVDQuartets remains theoretically valid under this model means that it can be confidently applied to empirical problems for which gene flow is thought to have occurred between any pair of sister taxa. Although SVDQuartets sometimes requires a large amount of data when the underlying substitution model is complex, it appears to be statistically consistent even in these complicated scenarios. In practice, bootstrap support values would provide a reasonable measure of uncertainty in the species tree estimate, and would be expected to be low when the amount of data was insufficient. In contrast, methods like ASTRAL and MP-EST could be statistically inconsistent, and bootstrap support values would likely not reflect this, because they assume an incorrect model (e.g., they

assume speciation with immediate cessation of gene flow and constant effective population size). Thus, ASTRAL and MP-EST could be said to be positively misleading, in the sense of [15], while SVDQuartets provides inference with an appropriate quantification of uncertainty.

Though we have focused our discussion largely on the effect of gene flow, we note that the model in Figure 1a generalizes previous species tree estimation frameworks by allowing variation in the effective population sizes, which determine the rate of coalescence across the species tree, even in the absence of gene flow. Further, we note that the results presented here concerning accuracy of the SVDQuartets method also apply to the case in which the species tree does not satisfy the molecular clock, following the arguments provided in [19]. Thus SVDQuartets holds under very general conditions, as it allows variation in effective population sizes across the species tree, violation of the molecular clock, and gene flow between sister taxa following speciation.

One natural extension of the model in Figure 1a is to allow gene flow between all pairs of taxa, including non-sisters. We have not yet considered this case, but speculate that certain choices of gene flow rates and effective population sizes might be problematic even for SVDQuartets, though this warrants further exploration. Though we consider here only the case of four-taxon species trees in our simulation studies, we note that for SVDQuartets this is sufficient, since the overall species-level phylogenetic estimate is obtained through assembly of the inferred relationships among quartets. For ASTRAL and MP-EST, however, we expect that difficulties in the four-taxon case will translate into reduced accuracy on larger trees, as well.

Models for estimation of species-level phylogenies based on data collected across the genome must necessarily try to incorporate realistic evolutionary mechanisms. By examining a model of speciation with gene flow, we have highlighted the complexity involved in using genealogical data to infer species-level relationships, as well as the impact that this complexity has on some of the commonly-used methods of species tree inference. Our finding that the method on which SVDQuartets is based holds for this more general model reinforces that this method is a valuable tool for estimating species trees from genome-scale data. Future work should continue to focus on improving the biological realism on which methods for species tree estimation are based.

REFERENCES

- [1] L. N. Andersen, T. Mailund, and A. Hobolth. Efficient computation in the IM model. *Journal of Mathematical Biology*, 68(6):1423–1451, 2014.
- [2] J. Chifman and L. Kubatko. Quartet inference from SNP data under the coalescent model. *Bioinformatics*, 30(23):3317–3324, 2014.
- [3] J. Chifman and L. Kubatko. Identifiability of the unrooted species tree topology under the coalescent model with time-reversible substitution processes, site-specific rate variation, and invariable sites. *Journal of Theoretical Biology*, 374:35–47, 2015.
- [4] Y. Chung and C. Ané. Comparing two Bayesian methods for gene tree / species tree reconstruction: A simulation with incomplete lineage sorting and horizontal gene transfer. *Systematic Biology*, 60(3):261–275, 2011.
- [5] J. Degnan and L. Salter. Gene tree distributions under the coalescent process. *Evolution*, 59:24–37, 2005.
- [6] A. J. Eckert and B. C. Carstens. Does gene flow destroy phylogenetic signal? the performance of three methods for estimating species phylogenies in the presence of gene flow. *Molecular Phylogenetics and Evolution*, 49(3):832–842, 2008.
- [7] J. Heled and A. J. Drummond. Bayesian inference of species trees from multilocus data. *Molecular Biology and Evolution*, 27(3):570–580, 2010.
- [8] J. Hey. Isolation with migration models for more than two populations. *Molecular Biology and Evolution*, 27(4):905–920, 2010.
- [9] J. Hey and R. Nielsen. Multilocus methods for estimating population sizes, migration rates and divergence time, with applications to the divergence of *Drosophila pseudoobscura* and *D. persimilis*. *Genetics*, 167:747–760, 2004.
- [10] A. Hobolth, L. N. Andersen, and T. Mailund. On computing the coalescence time density in an isolation-with-migration model with few samples. *Genetics*, 187(4):1241–1243, 2011.

- [11] H. Huang and L. L. Knowles. What is the danger of the anomaly zone for empirical phylogenetics? *Systematic Biology*, 58(5):527–536, 2009.
- [12] R. R. Hudson. Generating samples under a Wright–Fisher neutral model of genetic variation. *Bioinformatics*, 18(2):337–338, 2002.
- [13] T. Jukes and C. R. Cantor. Evolution of protein molecules. In H. N. Munro, editor, *Mammalian protein metabolism*, pages 21–123. Academic Press, New York, 1969.
- [14] S. Karlin and H. M. Taylor. *A First Course in Stochastic Processes*. Elsevier, second edition, 1975.
- [15] L. Kubatko and J. Degnan. Inconsistency of phylogenetic estimates from concatenated data under coalescence. *Systematic Biology*, 56:17–24, 2007.
- [16] A. D. Leaché, R. B. Harris, B. B. Rannala, and Z. Yang. The influence of gene flow on species tree estimation: A simulation study. *Systematic Biology*, 63:17–30, 2014.
- [17] L. Liu, L. Yu, and S. V. Edwards. A maximum pseudo-likelihood approach for estimating species trees under the coalescent model. *BMC Evolutionary Biology*, 10(1):302, 2010.
- [18] L. Liu, L. Yu, L. Kubatko, D. K. Pearl, and S. V. Edwards. Coalescent methods for estimating multilocus phylogenetic trees. *Molecular Phylogenetics and Evolution*, 53:320–328, 2009.
- [19] C. L. Long and L. S. Kubatko. Identifiability and reconstructibility of species phylogenies under a modified coalescent. *Bulletin of Mathematical Biology, in revision*, 2017.
- [20] S. Mirarab, R. Reaz, M. S. Bayzid, T. Zimmermann, M. S. Swenson, and T. Warnow. ASTRAL: Genome-scale coalescent-based species tree estimation. *Bioinformatics*, 30(17):i541–i548, 2014.
- [21] A. Rambaut and N. Grassly. SeqGen: An application for the Monte Carlo simulation of DNA sequence evolution along phylogenetic trees. *Computer Applications in Biosciences*, 13:235–238, 1997.
- [22] C. Solís-Lemus, M. Yang, and C. Ané. Inconsistency of species-tree methods under gene flow. *Systematic Biology*, 65(5):843–851, 2016.
- [23] S. Tavaré. Some probabilistic and statistical problems in the analysis of DNA sequences. *Lectures on Mathematics in the Life Sciences (American Mathematical Society)*, 17:57–86, 1986.
- [24] Y. Tian and L. Kubatko. Distribution of gene tree histories under the coalescent model with gene flow. *Molecular Phylogenetics and Evolution*, 105:177–192, 2016.
- [25] Y. Wang and J. Hey. Estimating divergence parameters with small samples from a large number of loci. *Genetics*, 184(2):363–379, 2010.
- [26] T. Zhu and Z. Yang. Maximum likelihood implementation of an isolation-with-migration model with three species for testing speciation with gene flow. *Molecular Biology and Evolution*, 29(10):3131–3142, 2012.